Available online at www.sciencedirect.com

ScienceDirect

Ceramics International 40 (2014) 1771–1779

CERAMICS INTERNATIONAL

www.elsevier.com/locate/ceramint

Low sintering temperature of $ZnNb_2O_6$ for silver co-sintering

Regis Quercioli, Jerome Bernard*, Jean-Marie Haussonne, Jean-Michel Reboul, David Houivet

Normandie University, ESIX, LUSAC, F-50130 Cherbourg-Octeville, France

Received 13 May 2013; received in revised form 5 July 2013; accepted 10 July 2013
Available online 22 July 2013

Abstract

The purpose of this study is the making of multilayer type I capacitors composed of $ZnNb_2O_6$ co-sintered with silver electrodes. In order to lower the sintering temperature, we have mixed three commercially available glass frit powders with $ZnNb_2O_6$. The sintering behaviours were studied by thermomechanical analysis (TMA). Two additives allowed us to sinter $ZnNb_2O_6$ at 900 °C. The sintered ceramic pellets show a type I dielectric behaviour close to the one of pure $ZnNb_2O_6$ (e.g.: dielectric constant around 22, resistivity above 10^{12} Ω. and dielectric losses lower than 10^{-3}). Ceramics were co-sintered with Ag in order to estimate Ag diffusion behaviour. One composition, $ZnNb_2O_6$+5 wt% (B_2O_3–ZnO–SiO_2) glass frit can be co-sintered at 900 °C with Ag electrodes and leads to type I dielectric properties.

Keywords: MLCC; Dielectric; Low sintering temperature; $ZnNb_2O_6$; Silver

1. Introduction

First investigated by Maeda et al. [1], $ZnNb_2O_6$ has the best dielectric properties (dielectric constant equals to 25 and high quality factor of 8370) among the isostructural orthorhombic columbite structure MNb_2O_6 (where M=Ca^{2+}, Co^{2+}, Mn^{2+} Ni^{2+} and Zn^{2+}) [2]. It may be very promising for microwave applications due to its very high quality factor. When applied to multilayer ceramic capacitors, on account of its high sintering temperature (around 1200 °C), inner electrodes must be Pd or at least a Pd/Ag alloy. Many efforts are devoted to eliminating Pd due to its high cost. Moreover Ag electrodes will own a better electrical conductivity which could improve capacitor electrical performances, notably ESR (Equivalent Series Resistance). It is thus necessary to sinter $ZnNb_2O_6$ at a temperature lower than 900 °C. Some additives were used in previous studies in order to lower the sintering temperature:

- CuO (5 wt% addition, sintering temperature 925 °C, ε_r=22, QF=59,500 GHz, τ_f=−66 ppm °C^{-1}) [3];
- V_2O_5–Bi_2O_3 (1 wt% V_2O_5+1 wt% Bi_2O_3 addition, sintering temperature 1000 °C, ε_r=22.9, tan(δ) < 10^{-3}) [4];
- V_2O_5–Bi_2O_3–CuO (1 wt% V_2O_5+1 wt% Bi_2O_3+2.5 wt% CuO addition, sintering temperature 880 °C, ε_r=23.4, QF=46,975 GHz, τ_f=−44.89 ppm °C^{-1}) [4] or (1.5 wt% add-on, sintering temperature 890 °C, ε_r=32.69, QF=67,100 GHz, τ_f=−32.69 ppm °C^{-1}) [5] or the same material but cosintered with pure Ag [6];
- B_2O_3–CuO (5 wt% CuO+2 wt% B_2O_3 addition, sintering temperature 900 °C, ε_r=22.5, QF=55,000 GHz, τ_f=−25 ppm °C^{-1}) [7]; and
- B_2O_3–ZnO–SiO_2 (5 wt% addition, sintering temperature 925/975 °C, ε_r=22.5/21.3, QF=12,800/38,000 GHz, τ_f=−69.6/−66.0 ppm °C^{-1}) [8].

Yet, in these literatures, Ag co-sintering was not performed [4,5,7,8], or microstructural and dielectric properties were not published [3,6].

We shall present here the sintering behaviour, the structural and microstructural analyses together with the electric and dielectric properties of ceramics and Ag co-sintered ceramics, composed of $ZnNb_2O_6$ mixed with commercial glass frits additives belonging to the composition diagrams B_2O_3–ZnO–SiO_2, B_2O_3–ZnO–Bi_2O_3 and B_2O_3–SiO_2–BaO and owning low softening points (T_g).

2. Experimental procedure

Stoechiometric $ZnNb_2O_6$ was synthesised by the conventional solid state route from high purity oxide ZnO (>99.8%) and Nb_2O_5 (99.5%). The starting materials were mixed and

*Corresponding author. Tel.: +33 233014553; fax: +33 233014235.
E-mail address: jerome.bernard@unicaen.fr (J. Bernard).

0272-8842/$ - see front matter © 2013 Elsevier Ltd and Techna Group S.r.l. All rights reserved.
http://dx.doi.org/10.1016/j.ceramint.2013.07.077

Table 1
Glass frit properties.

Ref.	Datasheet composition (wt%)	EDS (at%)	Calculated composition (wt%)	Density	S_{BET} (m^2/g)/ $Ø_{BET}$ (μm)	T_g (°C)	ε_r	Tan(δ) (%)	ρ (Ω cm)
BZBi	B_2O_3: 19.0 Bi_2O_3: 30–50 ZnO: 15–35 SiO_2: 1–10 Al_2O_3: 1–10	Bi: 20 Zn: 60 Si: 10 Al: 9	B_2O_3: 19.0 Bi_2O_3: 51 ZnO: 27 SiO_2: 3 Al_2O_3: 5	3.6	1.43/1.9	540	11.5	0.2	$> 10^{12}$
BZS	B_2O_3: 24.0 ZnO: 50–70 SiO_2: 2–15	Zn: 79 Si: 21	B_2O_3: 24.0 ZnO: 64 SiO_2: 12	5.1	0.16/6.0	640	10.2	10.0	$> 10^{12}$
BSBa	B_2O_3: 22.5 BaO: 30–50 SiO_2: 15–35 Al_2O_3: 2–15	Ba: 40 Si: 45 Al: 15	B_2O_3: 22.5 BaO: 46 SiO_2: 20 Al_2O_3: 11	3.7	4.10/0.4	673	1.0	7.0	$> 10^{12}$

ground in a high energy laboratory mill (Dyno-Mill Research Lab) with 0.8 mm diameter yttried zirconia balls during a normalised grinding time[1] of 6 min in 50 wt% charged aqueous solution. The powder was dried and calcined in air at 800 °C for 2 h to obtain the pure columbite $ZnNb_2O_6$ phase (JCPDF File no. 13-0473), identified by X-ray diffraction analysis using Cu-Kα radiation with an Inel Equinox 3000 curved detector diffractometer.

The powders were analysed by EDS (ThermoNoran) with a 3400 N Hitachi SEM, and BET specific surface measurements were made with a Micromeritics TriStarII. Glass frits were added to $ZnNb_2O_6$ with 5% in weight amounts and mixed by milling with a planetary mill (Pulverisette Fritsch P4) in an yttried zirconia bawl with 10 mm diameter balls (same material) for 20 min in ethanol. The densification behaviours of the mixed powders during the sintering cycle were recorded by dilatometric measurements performed in air with a TMA92 Setaram dilatometer with heating rate of 300 °C h^{-1}. Pellets with 10 mm diameter and around 1.5 mm thickness were formed by uniaxial pressing at 2000 kg cm^{-2}. The sintering was done in free atmosphere at 900 °C with heating and cooling rates of 150 °C h^{-1}, and different dwell times. During sintering, the pellets were placed on a bed of powder with the same composition. After sintering, samples were analysed by XRD and their density was measured with Micrometrics AccuPyc 1330 He pycnometer. Open porosity was estimated by calculating the ratio between He density and geometrical density. Disks were metalised on both faces with pure Ag ink and fired at 780 °C for 20 min in order to achieve a mechanical grip of the electrodes with the ceramic.

1 kHz and 1 V oscillation tension dielectric characterisations (C and tan δ) were performed with a RCL metre Fluke PM 6306 at 25 °C and moisture regulated to 10% (Secasi SLH100 hot/cold oven with regulated moisture rate). Temperature coefficients of dielectric constant (1 kHz, $V_{osc}=1$ V) were measured between −30 °C and +145 °C in Secasi SLH100. Insulation resistances were measured in a dry atmosphere (10% moisture) at 25 °C under a 1 V/μm DC bias (Sefelec M1500P megohmeter). The microwave properties were measured at ambient conditions (Agilent 8720ES Network Analyser).

[1]Defined by whole grinding time × grinding chamber's volume/whole volume of the slurry. It represents the effective grinding time for each individual powder grain in the slurry.

3. Results and discussion

3.1. Glass frit analyses

The commercial glass frit references will not be given. Instead, the following designations characterising glass frits compositions will be used: B for boron, Z for zinc, S for silicon, Bi for bismuth and Ba for barium.

Table 1 shows for each glass frit designation the compositions given by the producer's datasheet together with the EDS quantitative measurements (boron cannot be quantified with EDS) and the calculated composition, the density and the specific surface together with the calculated BET diameters (with the hypothesis of spherical particles). The deviation in diameter values is very important from a glass frit to another, some powders have very large grains in comparison with the initial $ZnNb_2O_6$ powder (density = 5.8, $S_{BET}=10.34$ m^2/g, and $Ø_{BET}=0.1$ μm). Although the granulometry between glass frits and the initial material are different, we achieve a homogeneous powder after grinding. Dielectric and resistivity measurements were performed on pure glass frits sintered 40 °C below T_g with 0.5 h dwell time.

3.2. Dilatometric study

The dilatometric measurements during sintering of pure $ZnNb_2O_6$ and compositions with different glass frit additions are gathered, Fig. 1. It appears that glass frits BZS and BZBi which contain both Boron and Zinc have a greater effect on the lowering of the sintering temperature compared to the BSBa glass frit. With BZS and BZBi glass frits we could expect to lower the sintering temperature below 900 °C, in order to be compatible with Ag electrodes co-sintering. BSBa addition has a limited effect, allowing only an optimal sintering temperature

close to 1050 °C. It appears that the low softening point is not correlated with the beginning of shrinkage. For BZBi and BZS softening points are respectively 540 °C and 640 °C, but the shrinkage only starts after 700 °C. The same phenomenon is observed for the last glass frit (BSBa): the softening point is 673 °C while the shrinkage occurs only at temperatures higher than 740 °C. So, the low softening point does not seem to be really influent but the presence of the two chemicals elements boron and zinc in the glass frit should be.

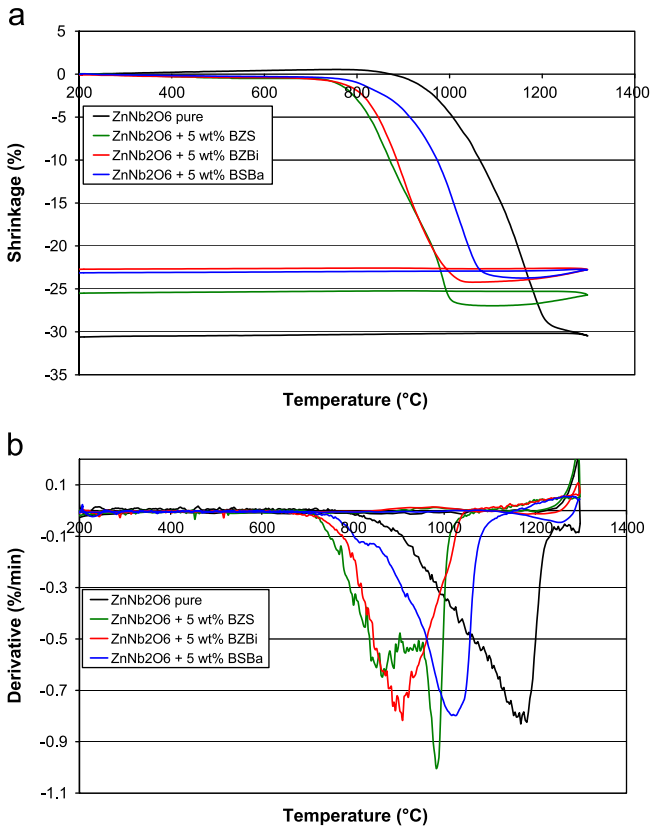

Fig. 1. Dilatometric behaviour of $ZnNb_2O_6$ with additives: (a) shrinkage behaviour and (b) shrinkage speed.

3.3. Samples characterisations

The XRD measurements (Fig. 2) performed on the surface of the pellets indicate the presence of a secondary phase for samples with BZS and BZBi glass frit addition and none with BSBa. One can notice that, whatever the composition of the glass frit is, $ZnNb_2O_6$ cell parameters are not modified even if substitutions may occur.

For the BZS addition, the secondary phase is Zn_2SiO_4 (ε_r=6.6 [9]) which may contribute to a slight lowering of ε_r. It is noteworthy that this secondary phase was not detected by Sanoj et al. [8] on a quite similar material ($ZnNb_2O_6$+5 wt% {60 wt% ZnO–30 wt% B_2O_3–10 wt% SiO_2 glass frit}).

For BZBi, the glass frit induced the formation of $BiNbO_4$ ($\varepsilon_r \approx 43$ [10]). This high dielectric constant will let us expect an increase in the dielectric constant of the pellet. Yet, the amount of secondary phase seems to be very low.

Microstructure observations and EDX analysis confirm the presence of the secondary phases detected with XRD measurements, but also reveal other secondary phases with BZBi and BSBa additions.

Samples with BZS show a darker secondary phase with BSE imaging (Fig. 3A), which was identified as Zn_2SiO_4 phase from semi-quantitative data obtained by EDX (presence of zinc and silicon with an atomic ratio Zn:Si close to 2:1). Calculated porosity from pictures is lower than 2% and is coherent with the porosity measured with He pycnometry.

Fig. 3B is a micrograph of a pellet sintered with BZBi glass frit. EDX analysis on bright areas suggests the presence of $BiNbO_4$ secondary phase together with $Zn_3Nb_2O_8$ (ε_r=21.6 [11]) for the small dark ones. This secondary phase was not detected by XRD analysis, since it was in too small amount to be detected. The image analysis (with ImageJ software) gives a

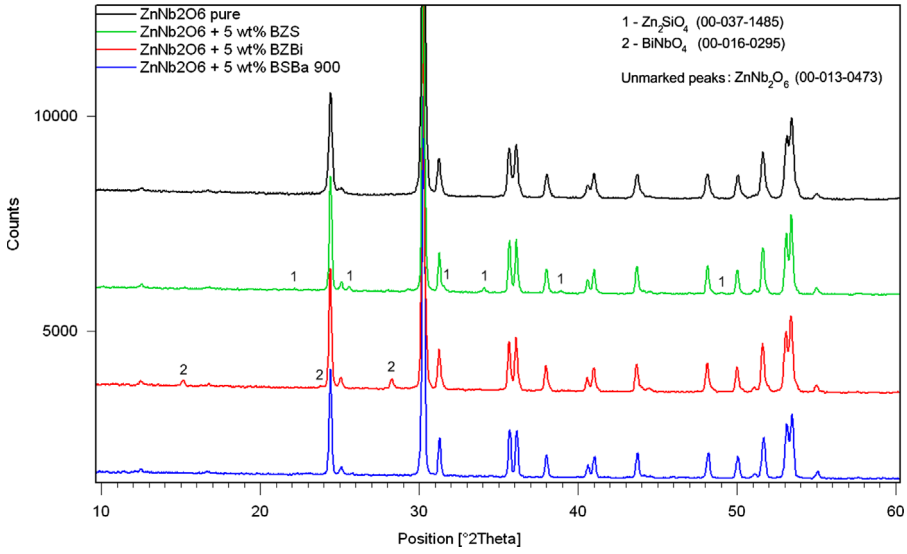

Fig. 2. Diffractograms of $ZnNb_2O_6$ sintered at 900 °C for 4 h with 5 wt% BZS and BZBi glass frit additions, for 8 h with 5 wt% BSBa glass frit addition.

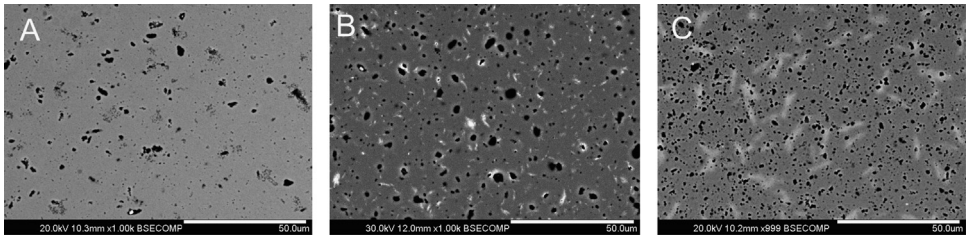

Fig. 3. Microstructure of (A) $ZnNb_2O_6$+5 wt% BZS, (B) $ZnNb_2O_6$+5 wt% BZBi, and (C) $ZnNb_2O_6$+5 wt% BSBa sintered at 900 °C for 4 h (A and B) or 8 h (C).

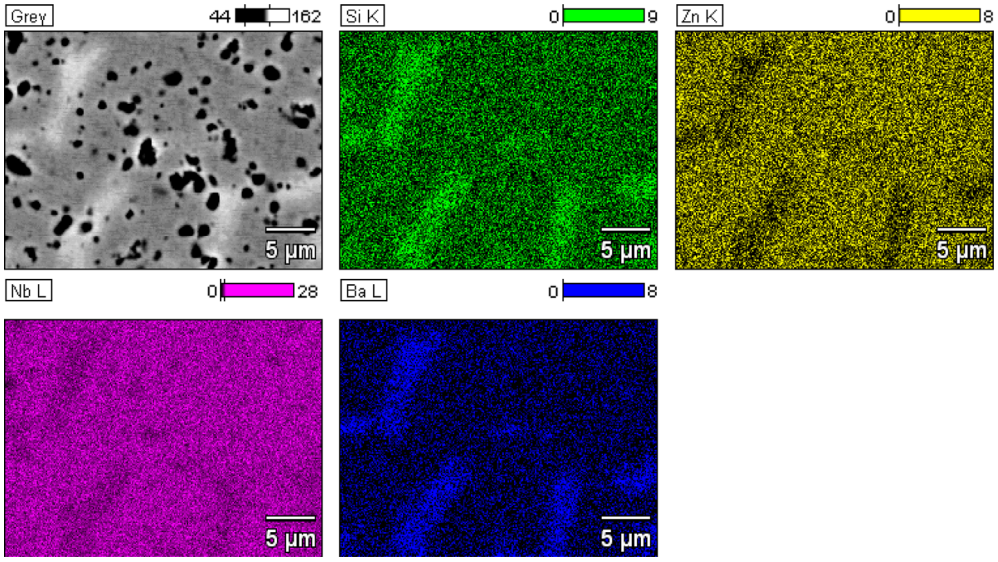

Fig. 4. Spectral imaging of $ZnNb_2O_6$+5 wt% BSBa sintered at 900 °C for 8 h.

Table 2
Pellet properties.

Sample ref.	Sintering temperature and dwell time	Shrinkage (%)	Open porosity (%)	ε_r	Tan(δ) (%)	ρ (Ω cm)	τ_ε (ppm °C^{-1})	QF (GHz) at 7.5 GHz
$ZnNb_2O_6$ pure	1150 °C – 2 h	17.5	≈2	24.0	< 0.1	> 10^{12}	+147	92,600
$ZnNb_2O_6$+5 wt% BZS	900 °C – 4 h	15.9	≈2	21.1	< 0.1	> 10^{12}	+147	23,070
$ZnNb_2O_6$+5 wt% BZBi	900 °C – 4 h	17.0	≈2	22.9	< 0.1	> 10^{12}	+146	18,230
$ZnNb_2O_6$+5 wt% BSBa	900 °C – 8 h	14.1	≈2	21.8	< 0.1	≈10^{12}	+135	12,640

porosity close to 5%, which is higher than He pycnometry porosity, this should be a closed porosity.

$ZnNb_2O_6$ with 5 wt% BSBa addition pellets (Fig. 3C) are characterised by elongated bright areas. As shown on spectral imaging (Fig. 4), bright diffuse areas have a composition rich in silicon and barium elements which is similar to the one of the BSBa glass frit (except for boron which could not be quantified with EDX measurement). It should be an amorphous phase as it has not been detected by XRD. The porosity is higher than 10%. As already supposed for BZBi samples, it should be a closed one.

Table 2 gives for each sample: its sintering temperature, dwell time, shrinkage rate, open porosity estimated from the He pycnometric volume, dielectric (ε_r, tan(δ), and τ_ε) and electrical (ρ) measurements. The sintering temperature was chosen in order to be compatible with silver cosintering. For $ZnNb_2O_6$+5 wt% BSBa which normally has to be sintered at higher temperature (1050 °C), a longer dwell time (8 h) allows a good densification but always slightly lower than the one observed with BZS and BZBi additions.

Among the elements present in the three glass frits, substitutions on A sites seem to be very difficult considering ionic radii with a coordination number of 6 (Nb^{5+} = 0.64 Å, Zn^{2+} = 0.74 Å, B^{3+} = 0.27 Å, Si^{4+} = 0.4 Å, Bi^{3+} = 1.03 Å, Ba^{2+} = 1.35 Å and Al^{3+} = 0.535 Å). But, Zn and Al can be considered to substitute Nb on B site of $ZnNb_2O_6$. For all the three materials (i.e. $ZnNb_2O_6$+5 wt% BZS, $ZnNb_2O_6$+5 wt% BZBi and $ZnNb_2O_6$+5 wt% BSBa), Zn:Nb ratio in primary phase is

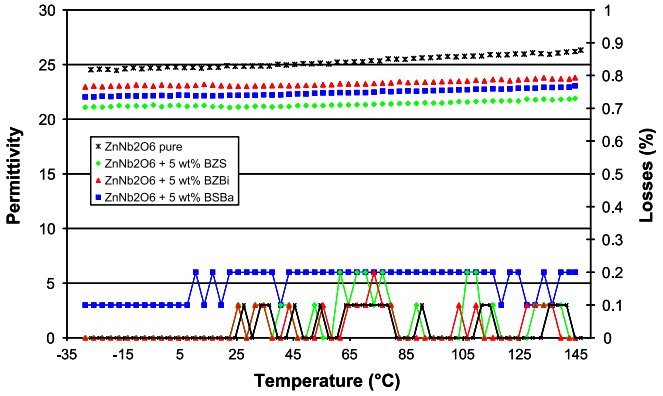

Fig. 5. Dielectric properties vs. temperature of ceramics without Ag co-sintering.

still close to 1:2. So if these substitutions occur they should be limited because they are not detected by XRD and EDX measurements. Even if limited, they should contribute to lowering the sintering temperature due to the appearance of oxygen vacancies on anionic lattice. On the other hand, boron can also contribute to this lowering [12].

These samples are all nearly full densified with only a very low estimated open porosity (lower than 2%). Electrical and dielectrical properties of pure $ZnNb_2O_6$ correspond to those found in the literature e.g.: $\varepsilon_r=24$, $\tan(\delta)<0.1$, $\rho>10^{12}\,\Omega$ cm [2,13].

As expected, correlated with the presence of the low permittivity Zn_2SiO_4 (ε_r=6.6) secondary phase, samples with BZS belong to a ε_r lower than the one of pure $ZnNb_2O_6$. Contrariwise, BZBi glass frit additions do not lead to a higher ε_r in spite of the presence of a secondary phase with ε_r=43. Maybe its effects are minored by the presence of $Zn_3Nb_2O_8$ and the 5% porosity. Dielectric losses remain very low ($<0.1\%$) for all samples, and resistivity is above $10^{12}\,\Omega$ cm. Secondary phases are not detrimental to $ZnNb_2O_6$ properties but affect the microwave properties. For BSBa glass frit addition, we observe a decrease of the resistivity. For the three additions, dielectric constants and losses are stable in temperature (Fig. 5). The electrical and dielectric properties of all these compositions are compatible with type I dielectric applications. All of them have a positive Temperature Coefficient of Permittivity close to 140 ppm $^{\circ}C^{-1}$.

3.4. Ag electrode co-sintering

All the glass frits used in this work can allow $ZnNb_2O_6$ to be sintered at a temperature compatible with Ag electrode. Whatever the composition is, linescans EDX analysis made at the Ag/ceramic interface (Fig. 6) do not reveal any Ag diffusion in $ZnNb_2O_6$ as the composition profile is sharp (if taking in consideration the size of the electron beam).

Compositions with BZS glass frit have the same secondary phase when sintered alone or co-sintered with Ag, when analysed with XRD and SEM (Fig. 7). Moreover, their electrical and dielectrical properties remain very close in both cases.

When co-sintered with an Ag layer, the composition with BZBi additive contents a secondary phase different to the one indentified when sintered alone as illustrated in Fig. 8. The secondary phase of co-sintered samples owns a pyrochlore crystalline structure close to the one of $(Bi_{0.75}Zn_{0.25})_2(Nb_{0.75}Zn_{0.25})_2O_7$ (JPDF File no. 54-0971).

SEM observations do not reveal pure Ag in the thickness of the samples but show the presence of very bright areas located around the pores (Fig. 9). The EDX analysis of these areas reveals the presence of Ag, Zn, Nb and Bi. The element ratio is as follows: Zn: 14 at%, Nb: 48 at%, Ag: 16 at% and Bi: 22 at %. On the left of Fig. 9 (up side is Ag electrode), it can be seen that the areas' size of this phase is not homogeneous along the pellet's thickness (≈1.1 mm) but the Ag concentration in these bright areas is nearly constant in the entire sample. It seems that Ag diffusion took place through a porous medium and that it concentrates in this new secondary phase. As this phase migrates easily in the material, we can consider that it may be involved in the sintering mechanisms. When located in A site of the pyrochlore cell with a coordination number of 8, Ag^+ has a radius of 1.28 Å so it can only substitute Bi^{3+} cation whose radius is 1.17 Å, but not Zn^{2+} which is 0.9 Å. Ag^+ with a coordination number of 6 has a radius of 1.15 Å; so it cannot substitute neither Nb nor Zn on the B site as Nb^{5+} and Zn^{2+} have a ionic radius respectively equal to 0.64 Å and 0.74 Å. Only a substitution of Bi by Ag should be possible in this secondary phase, which formula should be then close to $(Bi_{0.75-x}Ag_xZn_{0.25})_2(Nb_{0.75}Zn_{0.25})_2O_{7-2x}$. Oxygen defect can lead to a smaller cell parameter of the structure which could explain a shift of the peaks numbered "1" toward high angle of the diffractogram in regard of the reference datasheet (JPDF File no. 54-0971).

The electrical and dielectric measurements of these samples show a high dielectric constant (ε_r=25.5), a resistivity above $10^{12}\,\Omega$ cm, but important losses ($\tan(\delta)\approx0.5\%$). As bismuth based pyrochlores, without Ag, have good dielectric properties [13,14], these losses could be correlated to Bi substitutions by Ag in this secondary phase which lead to vacancies on the anionic network and could induce an ionic conduction.

$ZnNb_2O_6$ with BSBa additive pellets sintered without Ag had a secondary phase, not detectable by XRD but only observed with SEM, rich in Ba and Si elements. When co-sintered with an Ag electrode, XRD measurements show two new secondary phases (Fig. 10): Zn_2SiO_4 and a phase isomorphic to $Ba_2NaNb_5O_{15}$ (00-040-1463) which has a tetragonal bronze tungsten crystalline structure.

SEM BSE/EDX microstructural analyses do not show any presence of pure Ag in bulk but clearly indicate that three different phases co-exist (Fig. 11). The composition of the dark grey areas is close to the one of Zn_2SiO_4, while the light ones are characterised by the following elements ratio: Nb:49 at%, Ag:12 at% and Ba:18 at%. As for Ag co-sintered pellets made with $ZnNb_2O_6$+5 wt% BZBi, left part of Fig. 11 (Ag electrode on top) shows that this new phase has an inhomogeneous size along the sample's thickness (≈1 mm). In this bright phase, Ag concentration is nearly constant in all the sample thickness and it seems that Ag diffusion still took place through a medium of pores and concentrates in this new secondary phase. This phase migrates easily in the material too, so we can also

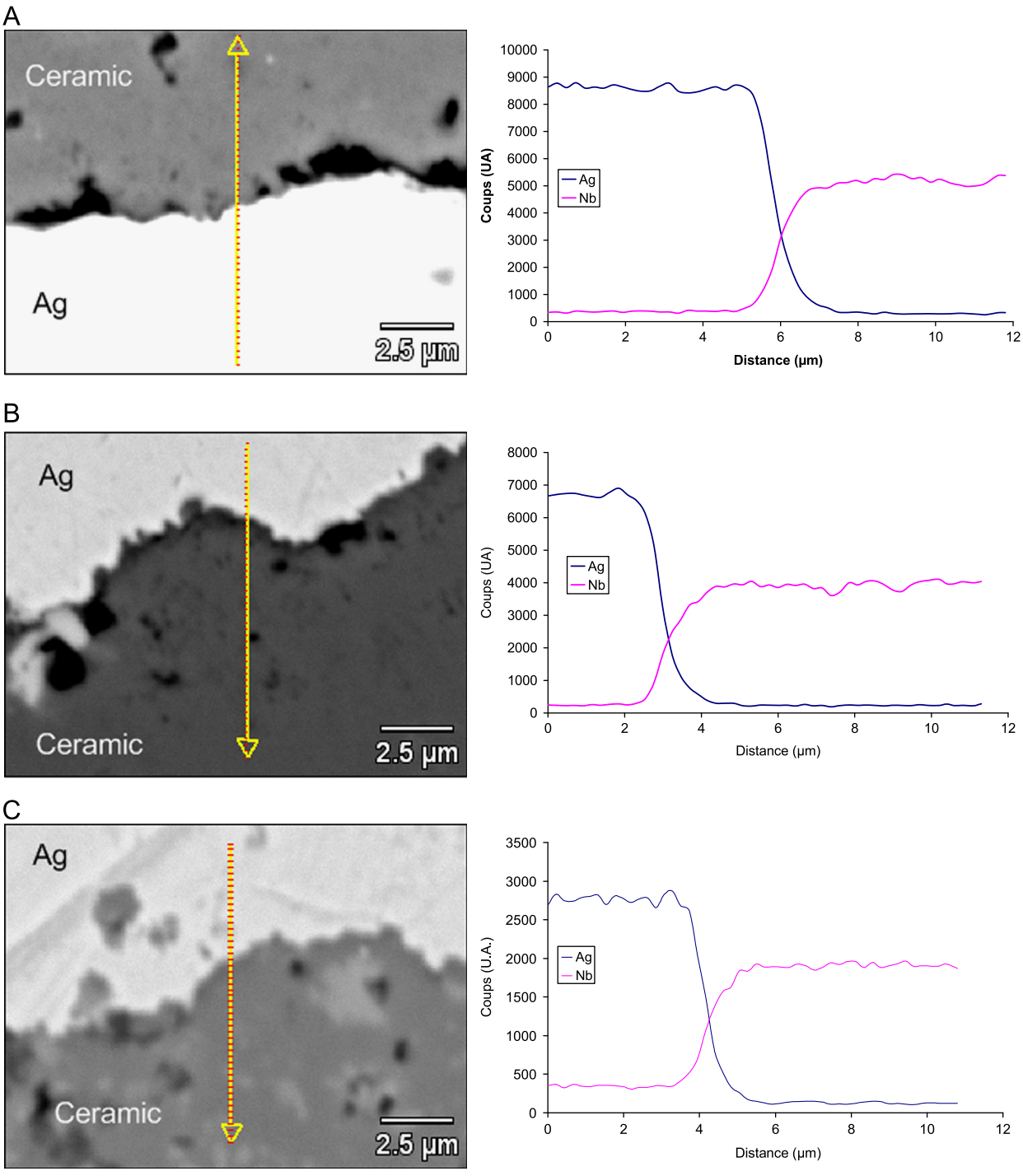

Fig. 6. Ag co-sintered samples profiles. (a) $ZnNb_2O_6$+5 wt% BZs, (b) $ZnNb_2O_6$+5 wt% BZBi and (c) $ZnNb_2O_6$+5 wt% BSBa.

consider that it is involved in the sintering mechanisms. Considering diffractogram and atomic quantification in the bright areas, this secondary phase should be $Ba_2AgNb_5O_{15}$. Medium grey area is $ZnNb_2O_6$ with a zinc deficit (Zn: 31 at% and Nb: 69 at%). Missing Zn should have migrated to form the dark grey secondary phase Zn_2SiO_4.

When compared to samples sintered without Ag, these samples have a lower permittivity ($\varepsilon_r = 20.3$), lower losses ($\tan(\delta) < 0.1\%$) and a higher resistivity ($\rho > 10^{12}\ \Omega\,cm$). Ag co-sintering seems to improve some characteristics of this material, but Ag detected in bright areas could be detrimental to breakdown electric field [15] and to life span [16] of components made with this composition.

Permittivity and dielectrical losses measurements vs. temperature have been done for Ag co-sintered pellets (Fig. 12).

$ZnNb_2O_6$+5 wt% BZBi material has its permittivity and losses values increasing with the temperature showing the existence of semi-conduction. This result is in good agreement

with the assumption previously made about a possible ionic conduction due to anionic vacancies because of the substitution of Bi by Ag in the pyrochlore secondary phase.

Contrariwise, when compared to non-co-sintered samples, it can be observed that Ag co-sintered $ZnNb_2O_6$ with BZS or BSBa glass frit additions have the same behaviour when measured from −32 °C to +145 °C: they are still class I dielectric materials.

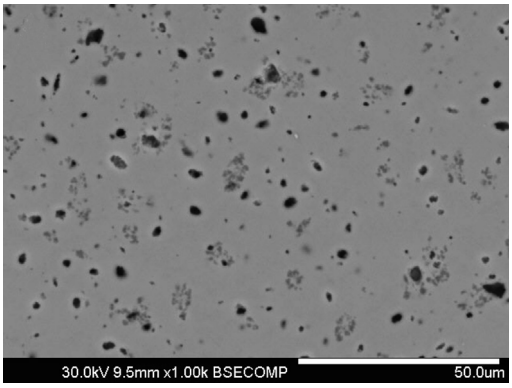

Fig. 7. Microstructure of $ZnNb_2O_6$+5 wt% BZS Ag co-sintered at 900 °C for 4 h.

4. Conclusions

Commercial glass frits additives based on B_2O_3–ZnO–SiO_2, B_2O_3–ZnO–Bi_2O_3 and B_2O_3–SiO_2–BaO can sufficiently lower the sintering temperature of $ZnNb_2O_6$ to make it compatible with Ag electrodes for LTCC applications. Moreover, in the case of BZS additions, we have shown with comparison to the literature the ability to lower the sintering temperature to 900 °C together with the obtaining of improved microwave properties (QF = 23,070 GHz at 900 °C instead of QF = 12,800 GHz at 925 °C [8]).

The material based on BZBi glass frit owns as well good electric and dielectric characteristics. But, when co-sintered with Ag, the presence of a secondary phase (containing Ag) induced in this case high dielectric losses.

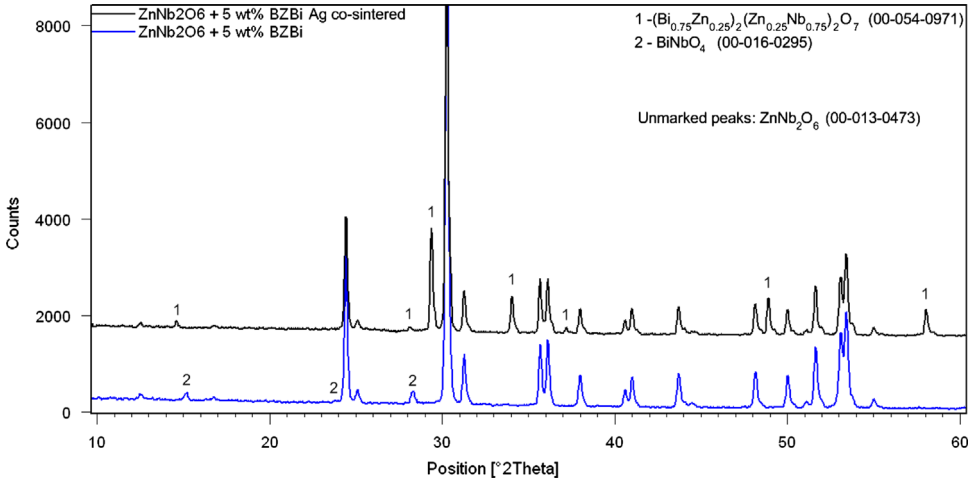

Fig. 8. $ZnNb_2O_6$+5 wt% BZBi diffractograms of ceramics sintered alone or co-sintered with Ag at 900 °C for 4 h.

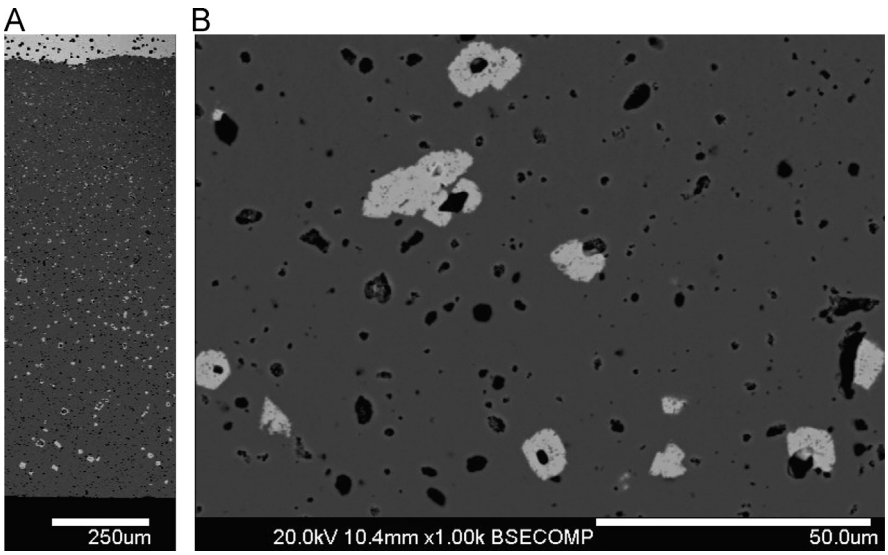

Fig. 9. Evolution of microstructure of $ZnNb_2O_6$+5 wt% BZBi Ag co-sintered at 900 °C for 4 h, between Ag electrode and surface of sample (A: general view and B: detail).

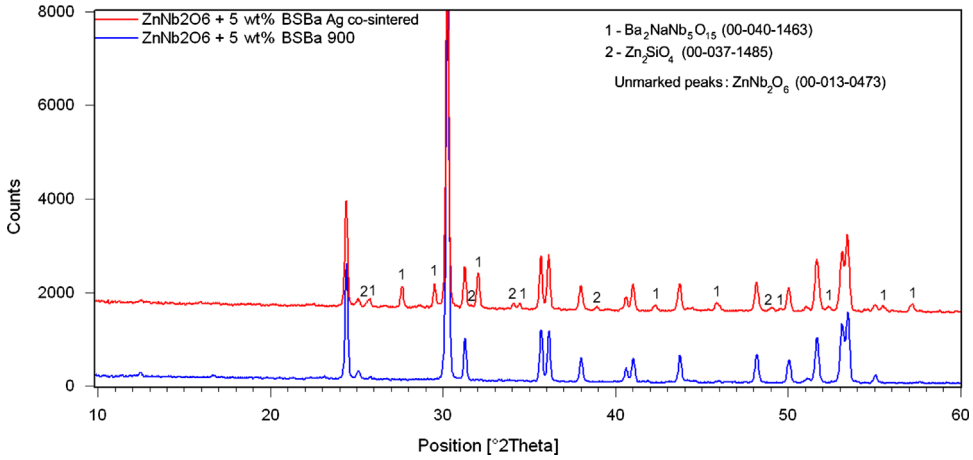

Fig. 10. $ZnNb_2O_6$+5 wt% BSBa diffractograms of ceramics sintered alone or co-sintered with Ag at 900 °C for 8 h.

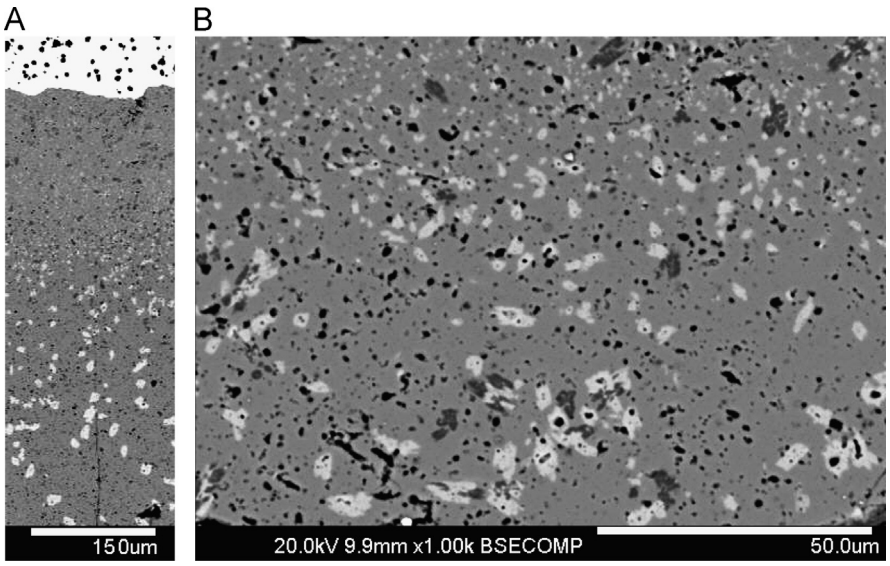

Fig. 11. Evolution of microstructure of $ZnNb_2O_6$+5 wt% BSBa Ag co-sintered at 900 °C for 8 h, between Ag electrode and surface of sample (A: general view and B: detail).

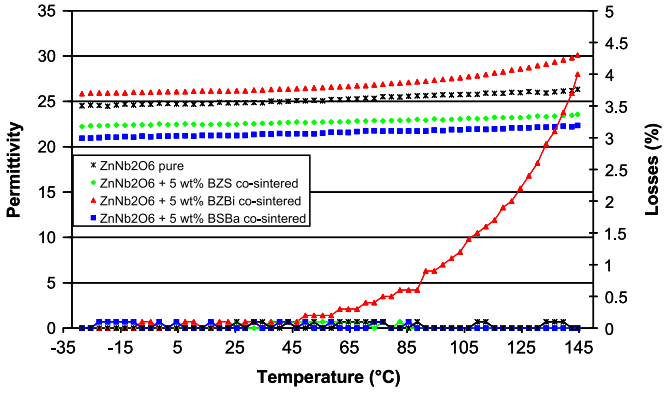

Fig. 12. Dielectric properties vs. temperature of pellets co-sintered with Ag.

For BSBa glass frit addition we also observe type I properties even when Ag co-sintered samples have good properties, nonetheless Ag presence in one of the two secondary phases.

From the three studied compositions, $ZnNb_2O_6$+5 wt% BZS is the one with the best electric and dielectric properties: $\varepsilon_r = 21.1$, $\tan(\delta) < 0.1$, $\rho > 10^{12}\ \Omega$ cm, $\tau_\varepsilon = +147$ ppm °C^{-1}, $QF = 23{,}070$ GHz when sintered at 900 °C for 1 h alone or co-sintered with Ag. With this material type I MLCC with Ag inner electrodes can be considered. We are now studying the aging behaviour under electric field and proceeding climatic studies of multilayer capacitors prototypes.

This study is part of ANR-08-MAPR-0013 project "Cheapcomponents".

We wish to thank our industrial partner: TEMEX Ceramics.

References

[1] M. Maeda, T. Yamamura, T. Ikeda, Dielectric characteristics of several complex oxide ceramics at microwave frequencies, Japanese Journal of Applied Physics 26 (1987) 76–79.

[2] H. Lee, K. Hong, S. Kim, I. Kim, Dielectric properties of MNb_2O_6 compounds (where M=Ca, Mn, Co, Ni, or Zn), Materials Research Bulletin 32 (1997) 847–855.

[3] D.W. Kim, K.H. Ko, K.S. Hong, Influence of copper(II) oxide additions to zinc niobate microwave ceramics on sintering temperature and dielectric properties, Journal of the American Ceramic Society 84 (2001) 1286–1290.
[4] F. Gao, J. Liu, R. Hong, Z. Li, C. Tian, Microstructure and dielectric properties of low temperature sintered $ZnNb_2O_6$ microwave ceramics, Ceramics International 35 (2009) 2687–2692.
[5] Y.C. Zhang, L.T. Li, Z.X. Yue, Z.L. Gui, Effects of additives on microstructures and microwave dielectric properties of $ZnNb_2O_6$ ceramics, Materials Science and Engineering B 99 (2003) 282–285.
[6] Y.C. Zhang, Z.X. Yue, Z.L. Gui, L.T. Li, Microwave dielectric properties of $CuO–V_2O_5–Bi_2O_3$-doped $ZnNb_2O_6$ ceramics with low sintering temperature, Journal of Electroceramics 14 (2005) 67–74.
[7] C. Huang, R. Lin, J. Wang, Effect of B_2O_3 additives on sintering and microwave dielectric behaviors of CuO-doped $ZnNb_2O_6$ ceramics, Japanese Journal of Applied Physics 41 (2002) 758–762.
[8] M.A. Sanoj, C.P. Reshmi, M.R. Varma, Finite size effect on the sinterability and dielectric properties of $ZnNb_2O_6$–ZBS glass composites, Journal of the American Ceramic Society 92 (2009) 2648–2653.
[9] Y. Guo, H. Ohsato, K. Kakimoto, Characterization and dielectric behavior of willemite and TiO_2-doped willemite ceramics at millimeter-wave frequency, Journal of the European Ceramic Society 26 (2006) 1827–1830.
[10] H. Kagata, T. Inoue, J. Kato, I. Kameyama, Low-fire bismuth-based dielectric ceramics for microwave use, Japanese Journal of Applied Physics 31 (1992) 3152–3155.
[11] D.W. Kim, J.H. Kim, J.R. Kim, K.S. Hong, Phase constitutions and microwave dielectric properties of $Zn_3Nb_2O_8–TiO_2$, Japanese Journal of Applied Physics 40 (2001) 5994–5998.
[12] S. d'Astorg, S. Marinel, O. Perez, A. Veres, Investigation of some niobate-based dielectrics in view of base metal co-sintering, Journal of the European Ceramic Society 27 (2007) 4445–4451.
[13] D.P. Cann, C.A. Randall, T.R. Shrout, Investigation of the dielectric properties of bismuth pyrochlores, Solid State Communications 100 (1996) 529–534.
[14] X. Wang, H. Wang, X. Yao, Structures, phase transformations, and dielectric properties of pyrochlores containing bismuth, Journal of the American Ceramic Society 80 (1997) 2745–2748.
[15] Y. Lee, Dielectric properties and reliability of $Zn_{0.95}Mg_{0.05}TiO_3$+0.25-TiO_2 MLCCs with different Pd/Ag ratios of electrodes, International Journal of Applied Ceramic Technology 7 (2010) 71–80.
[16] W. Lee, C. Su, Y.C. Lee, J. Yang, T. Yang, S. PinLin, Effect of inner electrode on reliability of (Zn,Mg)TiO_3-based multilayer ceramic capacitor, Japanese Journal of Applied Physics 45 (2006) 5859–5864.